



# RESEARCH MEMORANDUM

ENGINEERING DEPT. LIBRARY

CHANGE VOLUNT AIRCRAFT

WASHINGTON, D.C.

CALCULATIONS OF THE SUPERSONIC WAVE DRAG OF NONLIFTING WINGS  
WITH ARBITRARY SWEEPBACK AND ASPECT RATIO

WINGS SWEPT BEHIND THE MACH LINES

By

Sidney M. Harmon and Margaret D. Swanson

Langley Memorial Aeronautical Laboratory  
Langley Field, Va.

CLASSIFIED DOCUMENT

This document contains classified information affecting the National Defense of the United States within the meaning of the Espionage Act, USC 50:31 and the transmission or the revelation of its contents in any manner to an unauthorized person is prohibited by law.

Information classified may be imparted only to persons in the military and naval services of the United States, appropriate civilians, officers and employees of the Federal Government who have a legitimate interest therein and to United States citizens of known loyalty and discretion who of necessity must be informed thereof.

CLASSIFICATION CHANGED TO *Unclassified*  
BY AUTHORITY OF *NASA Bulletin #122*  
ON *10/18/66* *ORJSC*

## NATIONAL ADVISORY COMMITTEE FOR AERONAUTICS

WASHINGTON

February 21, 1947

*3/5/47*

NATIONAL ADVISORY COMMITTEE FOR AERONAUTICS

RESEARCH MEMORANDUM

CALCULATIONS OF THE SUPERSONIC WAVE DRAG OF NONLIFTING WINGS

WITH ARBITRARY SWEEPBACK AND ASPECT RATIO

WINGS SWEEPED BEHIND THE MACH LINES

By Sidney M. Harmon and Margaret D. Swanson

SUMMARY

On the basis of a recently developed theory for finite swept-back wings at supersonic speeds, calculations of the supersonic wave drag at zero lift were made for a series of wings having thin symmetrical biconvex sections with untapered plan forms and various angles of sweepback and aspect ratios. The results are presented in a unified form so that a single chart permits the direct determination of the wave drag for this family of airfoils for an extensive range of aspect ratio and sweepback angle for stream Mach numbers up to a value corresponding to that at which the Mach line coincides with the wing leading edge.

The calculations showed that in general the wave-drag coefficient decreased with increasing sweepback. At Mach numbers for which the Mach lines are appreciably ahead of the wing leading edge, the wave-drag coefficient decreased to an important extent with increases in aspect ratio or slenderness ratio. At Mach numbers for which the Mach lines approach the wing leading edge (Mach numbers approaching a value equal to the secant of the angle of sweepback), the wave-drag coefficient decreased with reductions in aspect ratio or slenderness ratio. In order to check the results obtained by the theory, a comparison was made with the results of tests at the Langley Memorial Aeronautical Laboratory of swept-back wing attached to a freely falling body. The variation of the drag with Mach number and aspect ratio as given by the theory appeared to be in reasonable agreement with experiments for the range of Mach number tested.

INTRODUCTION

Recent developments in airfoil theory for supersonic speeds (references 1 and 2) indicate pronounced effects of sweepback and

aspect ratio on the drag. In reference 1, a theory was developed for calculating the pressure distribution at supersonic speeds and zero lift for swept-back wings of arbitrary linear taper and aspect ratio having thin symmetrical airfoil sections of sharp leading edges.

In the present paper, the method of reference 1 is applied to calculate the supersonic wave drag for a series of wings having thin symmetrical biconvex sections at zero lift with untapered plan forms and various angles of sweepback and aspect ratios. The term "biconvex profile" as used herein refers to an airfoil section composed of two parabolic arcs. In each case, the wing is considered to be cut off in a direction parallel to the direction of flight. In the calculations the Mach number is varied from 1.0 to a value corresponding to that at which the Mach line coincides with the wing leading edge. The results of the calculations are presented in a unified form which permits the direct determination from a single chart of the wave drag for this family of wings for an extensive range of sweepback angle and aspect ratio for Mach numbers from 1.0 to the value corresponding to that at which the Mach line coincides with the wing leading edge, or equal to the secant of the angle of sweepback. Although the calculations have been made for the biconvex profile, the data may be applied to indicate corresponding results for profiles approximately similar to the biconvex.

In order to illustrate the possible applicability of the theory to a typical swept-back wing, the calculated drag of a wing of  $45^\circ$  sweepback at zero lift is compared with the results of tests made at supersonic speeds at the Langley Memorial Aeronautical Laboratory on swept-back wings attached to a freely falling body.

#### SYMBOLS

$x, y, z$	coordinates of mutually perpendicular system of axis in wing
$dz/dx$	slope of airfoil surface
$c$	chord of airfoil section, measured in flight direction
$t/c$	thickness ratio of section, measured in flight direction
$\Lambda$	angle of sweep, degrees
$m = \cot \Lambda$	

- h wing semispan measured along y-axis, semichords except in appendix A
- K parameter indicating spanwise position equal to  $y/m$ , semichords
- A aspect ratio
- $l/t$  slenderness ratio, ratio of wing semispan measured along leading edge to maximum thickness of center section
- p disturbance pressure
- $p/q$  pressure coefficient, ratio of disturbance pressure to dynamic pressure in free stream
- V velocity in flight direction
- u x-component of disturbance velocity, positive in flight direction
- $\bar{u}$  u caused by source line with reversal in sign of m
- w z-component of disturbance velocity
- $\phi$  disturbance-velocity potential
- I source factor required to maintain a given wedge angle
- M Mach number
- $\beta = \sqrt{M^2 - 1}$
- $y_a$  coordinate measured along y-axis which is shifted to tip section, semichords
- $y_b$  coordinate measured along y-axis which is shifted to opposite tip section, semichords
- d wave drag at section
- $c_{d_\infty}$  wave-drag coefficient at section without tip effect
- $c_d$  wave-drag coefficient at section including tip effect
- $\Delta c_d$  increment in section wave-drag coefficient caused by wing tips

- $\Delta c_{dI}$  increment in section wave-drag coefficient caused by wing tip located on same half of wing as section
- $\Delta c_{dII}$  increment in wave-drag coefficient at section on one wing panel caused by tip of opposite wing panel
- $C_{D\infty}$  wave-drag coefficient for wing without tip effect
- $C_D$  wave-drag coefficient for wing including tip effect
- $\Delta C_D$  increment in wave-drag coefficient caused by tips, complete wing
- $\Delta C_{DI}$  increment in wave-drag coefficient on one wing panel caused by adjacent wing tip, complete wing
- $\Delta C_{DII}$  increment in wave-drag coefficient on one wing panel caused by tip of opposite wing panel, complete wing
- $C_{DT}$  drag coefficient obtained as sum of coefficients for wave drag and friction drag
- $\xi, \eta$  auxiliary variables which replace  $x$  and  $y$ , respectively, used to indicate origin of source line

Primed values of  $A, y, y_a, y_b, h, m, dz/dx$ , and  $z$  indicate transformation involving multiplication by factor  $\beta$

Subscripts:

- 1, 2 wings related according to transformation which makes  $y\beta$  and  $m\beta$  equal respectively for two wings.

Subscript notations for  $u$  and  $\bar{u}$  indicate the origin of source line in terms of coordinates  $x$  and  $y$ , respectively

## ANALYSIS

Basic data.- The present analysis is based on thin-airfoil theory for small pressure disturbances and a constant velocity of sound throughout the fluid. The axes used are the mutually perpendicular  $x, y, z$  system in which the  $x$ -axis is taken in the direction of flight positive to the rear, the  $y$ -axis is along the

span positive to the right, and the z-axis is positive upwards. Figure 1 shows the symbols used to designate the wing-plan-form parameters. The present analysis is made for untapered wings of biconvex profile at zero lift and is limited to a Mach number range from 1.0 to the value corresponding to that at which the Mach line coincides with the wing leading edge, that is, to a value equal to the secant of the angle of sweepback.

Theory.- If  $p$  is the disturbance pressure computed for one surface of the airfoil section, the wave drag for the section is

$$d = 2 \int_0^c p \frac{dz}{dx} dx \quad (1)$$

and the section wave-drag coefficient

$$c_d = \frac{2}{c} \int_0^c \frac{p}{q} \frac{dz}{dx} dx \quad (2)$$

where  $dz/dx$  is the slope of the surface of the airfoil at the point  $x$ . For the symmetrical biconvex profiles (composed of parabolic arcs)

$$\frac{dz}{dx} \approx \frac{t}{c} \left( \frac{c}{2} - x \right)$$

where the thickness ratio  $t/c$  may be considered the sole shape parameter. From thin-airfoil theory,

$$\frac{p}{q} = - \frac{2}{V} \frac{\partial \phi}{\partial x} = \frac{2u}{V}$$

where  $u$  is the disturbance-velocity component in the  $x$ -direction, taken positive in the flight direction. For a given swept-back wing with  $\Lambda = \cot^{-1} m$ , the drag coefficient in equation (2) at the spanwise station  $y$  may now be written as

$$c_d(y) = \frac{16\frac{t}{c}}{c^2} \int_{y/m}^{\frac{y}{m}+c} u \left( \frac{c}{2} - x + \frac{y}{m} \right) dx \quad (3)$$

The desired integrand  $u$  in equation (3) may be determined by the procedure given in reference 1. On the basis of the linearized theory, reference 1 derives a solution representing an oblique (swept-back) source line making the angle of sweepback  $\Lambda$  with the  $y$ -axis. This solution utilized for the pressure field or for the disturbance velocity is the real part of

$$u_{0,0} = I \cosh^{-1} \frac{x - m\beta^2 y}{\beta |y - mx|} \quad (4)$$

where the subscript notation indicates that the source line starts at the origin of coordinates ( $x = 0$ ,  $y = 0$ ). Equation (4) is shown in reference 1 to satisfy the boundary condition for a thin

oblique wedge making the half-angle  $\left( \frac{dz}{dx} \right)'$  in the transformed coordinate system of reference 1 ( $y' = y\beta$ ,  $z' = z\beta$ ) where

$\left( \frac{dz}{dx} \right)' = \frac{w'}{V} = \frac{\pi}{V} \frac{\sqrt{1 - m'^2}}{m'} I$ . In order to obtain an equal wedge angle in the physical coordinate system, the following relations between the transformed coordinates of reference 1 and the physical coordinates are used

$$m' = m\beta$$

$$w' = \frac{\partial \phi}{\partial z'}$$

$$w = \frac{\partial \phi}{\partial z}$$

where  $w'$  and  $w$  refer, respectively, to the vertical velocities in the transformed and physical coordinate systems. Thus

$$w = \frac{\partial \phi}{\partial z'} \frac{\partial z'}{\partial z} = w' \beta$$

The half-angle of the wedge is then determined as

$$\frac{dz}{dx} = \frac{w}{V} = \frac{\pi}{V} \frac{\sqrt{1 - m^2 \beta^2}}{m} I$$

or the required source factor in order to maintain the desired wedge angle is

$$I = \frac{V}{\pi} \frac{m}{\sqrt{1 - m^2 \beta^2}} \frac{dz}{dx} \quad (5)$$

By superposition of solutions of the wedge type, swept-back wings of desired profile shape and plan form can be built up (reference 1). In order to satisfy the boundary conditions over the surface of a biconvex wing, semi-infinite source lines of equal strength are placed along the leading and trailing edges beginning at the center section, in conjunction with a constant distribution of sink lines along the chord. At the tip, where the wing is cut off, reversed semi-infinite source and sink lines are distributed so as to cancel exactly the effect of those originating at the center section in the entire region of space outboard of the tip. In the present analysis, the tip is assumed to be cut off in the direction of flight. The term "tip effect" refers to the effect of this wing cut-off. The form of the integrand  $u$  for equation (3) is given in appendix A.

In calculating the wave drag over the wing, the disturbances due to the elementary sources and sinks are evidently limited to the regions enclosed by their Mach cones. Figure 2 shows the typical Mach lines originating from the source lines at the leading and trailing edges of the center and tip sections over a wing of



45° sweepback. Figure 2(a) shows the Mach lines for the infinitely long wing, and figure 2(b) includes the Mach lines starting from the tip section. In each case the disturbance over the wing caused by the leading- and trailing-edge source lines is limited to the region of the wing behind the corresponding Mach line. The regions affected by each of the Mach lines are indicated in figure 2(b) as regions I to IV. Region I represents the part of the wing affected by the sink line starting from the leading edge of the adjacent tip; region II represents the wing area affected by the sink line starting from the opposite tip. Region III is influenced by the source line starting at the leading edge of the center section and includes the entire wing; region IV is influenced by the source line starting at the trailing edge of the center section.

The resultant velocity  $u$  at a point on the wing is made of the component velocities caused by each of these source and sink lines where the influence of each component is restricted to the region behind its Mach line. The drag coefficient  $c_{d_{co}}$  is there-

fore obtained by evaluating in equation (3) the integrand  $u_{0,0}$  over the entire section (region III), the integrand  $u_{c,0}$  over part of the section included in region IV, and the integrands for the  $u$ -components caused by the sink distributions along the profile (fig. 2(b) and appendix A, equation (A2)). The drag coefficients  $\Delta c_{d_I}$  and  $\Delta c_{d_{II}}$  are obtained similarly by integrating along the section in the regions I and II, respectively, in addition to the integrations for the  $u$ -components caused by the source distributions along the profile (appendix A). The limits of integrations for  $x$  along the chord and for  $y$  along the span, which represent the boundaries for the regions of influence for the individual  $u$ -functions required for a biconvex profile, are given in the table in appendix A.

Formulas for section wave-drag coefficients.- The formulas for the section drag coefficients obtained by integration of the  $u$ -functions and by use of equation (3) are presented in appendix B. These formulas give expressions for the drag coefficient without the tip effect  $c_{d_{co}}$  and also the expressions for the increments in  $c_d$  caused by the tip effect  $\Delta c_d$ .

Wave-drag coefficients for complete wing.- In the present investigation the section drag coefficients expressed by the equations in appendix B were integrated graphically to obtain the results for the wing-drag coefficients. Subsequently, however,

analytical expressions for the integrations were obtained. These formulas for the wing-drag coefficients are presented in appendix B.

Drag coefficient of swept-back wing at Mach number of 1.0.-  
The solution of the equations for  $c_d$  given in appendix B shows that, for a symmetrical untapered finite swept-back wing at Mach number of 1.0 and zero lift, positive and negative infinite values for  $c_d$  are obtained at various sections of the wing. The integration over the wing of the limiting values for these infinite terms, however, gives zero. Although some sections of the wing have infinitely positive or negative drag, the total drag coefficient over the wing results in a finite value. The prediction of infinite values of drag at certain sections of the wing clearly violates at these sections the assumption of small disturbances from which the linearized theory is derived. The calculated values for the total drag coefficient at Mach number 1.0 are therefore questionable. The formulas for the total drag at Mach number 1.0 are presented in appendix B.

Conversion of drag solution to series of related wings.- An examination of equations (B1), (B3), and (B5) indicates that the drag solution obtained for one value of  $m$  and  $M$  may be applied directly to obtain the drag for a whole series of wings in which each wing is at a certain appropriate Mach number. (Equation (B1) is formed by adding expression (B1b) to the right-hand side of equation (B1a).) For example, equation (B1) may be expressed in the following form:

$$c_{d_{\infty}}(y) = \frac{8}{\pi} \left(\frac{t}{c}\right)^2 \frac{m\beta}{\beta} F\left(\frac{y\beta}{m\beta}, m\beta\right) \quad (6)$$

where  $F\left(\frac{y\beta}{m\beta}, m\beta\right)$  refers to the variable terms and where  $m\beta = m'$ ,

and  $\frac{y}{m} = K$ . If the subscript 1 refers to a wing at Mach number corresponding to  $\beta_1$  and the subscript 2 to any other wing at the Mach number corresponding to  $\beta_2$ , then the drag coefficients for the two wings may be obtained from equation (6) as follows:

$$c_{d_{\infty 1}} = \frac{8}{\pi} \left(\frac{t}{c}\right)_1^2 \frac{m_1\beta_1}{\beta_1} F\left(\frac{y_1\beta_1}{m_1\beta_1}, m_1\beta_1\right) \quad (7a)$$

$$c_{d_{\omega_2}} = \frac{8}{\pi} \left(\frac{t}{c}\right)_2^2 \frac{m_2 \beta_2}{\beta_2} F\left(\frac{y_2 \beta_2}{m_2 \beta_2}, m_2 \beta_2\right) \quad (7b)$$

Equation (7) shows that if  $y_1 \beta_1 = y_2 \beta_2$  and  $m_1 \beta_1 = m_2 \beta_2$

$$c_{d_{\omega_1}} = c_{d_{\omega_2}} \frac{(t/c)_1^2 \beta_2}{(t/c)_2^2 \beta_1} = c_{d_{\omega_2}} \frac{(t/c)_1^2 \cot \Lambda_1}{(t/c)_2^2 \cot \Lambda_2} \quad (8)$$

where  $c_{d_{\omega_1}}$  and  $c_{d_{\omega_2}}$  refer to the spanwise positions  $y_1$  and

$\frac{y_1 \beta_1}{\beta_2}$ , respectively. In a similar manner, it can be shown that if

two wings are related according to  $y_1 \beta_1 = y_2 \beta_2$  and  $m_1 \beta_1 = m_2 \beta_2$ , the section drag coefficients obtained for wings 1 and 2 from equations (B3) and (B5) are in the same ratio as that expressed in equation (8). Equation (8), therefore, may be generalized to apply to the total drag coefficient at the section or,

$$c_{d_1} = c_{d_2} \frac{(t/c)_1^2 \cot \Lambda_1}{(t/c)_2^2 \cot \Lambda_2} \quad (9)$$

where  $c_{d_1}$  and  $c_{d_2}$  refer to the spanwise positions  $y_1$  and  $\frac{y_1 \beta_1}{\beta_2}$ , respectively.

The wing-drag coefficients for wings 1 and 2 are given, respectively, by

$$C_{D1} = \frac{1}{h_1} \int_0^{h_1} c_{d_1} dy_1 \quad (10)$$

$$C_{D_2} = \frac{1}{h_2} \int_0^{h_2} c_{d_2} dy_2 \quad (11)$$

By substituting for the integrand  $c_{d_1}$  in equation (10) the relationship expressed in equation (9) and by substituting  $\frac{dy_2 \beta_2}{\beta_1}$  for  $dy_1$ , equation (10) may be written as:

$$C_{D_1} = \frac{(t/c)_1^2 \cot \Lambda_1}{h_2 (t/c)_2^2 \cot \Lambda_2} \int_0^{h_2} c_{d_2} dy_2$$

or

$$C_{D_1} = C_{D_2} \frac{(t/c)_1^2 \cot \Lambda_1}{(t/c)_2^2 \cot \Lambda_2} \quad (12)$$

Equation (12) permits a rapid determination of the drag coefficient for wings of arbitrary sweepback, aspect ratio, and thickness ratio (within limitations of airfoil theory) from data obtained for one swept-back wing for the appropriate range of aspect ratio and Mach number. For this purpose, use of a wing of  $45^\circ$  sweepback as the reference wing is most convenient. If the subscript 2 is used to refer to the parameters for the wing of  $45^\circ$  sweepback and the subscript 1 is dropped, equation (12) becomes

$$C_D = \frac{C_{D_2} (t/c)^2 \cot \Lambda}{(t/c)_2^2} \quad (13)$$

where  $C_D$  and  $C_{D_2}$  refer to wings whose aspect ratios and Mach numbers are related by the following equations:

$$A_2 = A \tan \Lambda \quad (14)$$

$$\beta_2 = \beta \cot \Lambda \quad (15)$$

The foregoing analysis shows that the results obtained for a wing of  $45^\circ$  sweepback and a given aspect ratio  $A_2$  can be transformed by means of equation (13) to all wings for which the aspect-ratio parameter  $A \tan \Lambda = A_2$  and the Mach number parameter  $\beta \cot \Lambda = \beta_2$ .

The grouping of the parameters as indicated in the foregoing analysis permits the use of a single generalized chart for presenting the drag results. This chart is discussed in the section entitled "Results and Discussion."

Prandtl-Glauert rule modified for supersonic flows.- In considering the linearized problem of supersonic flow past a wing, it is often convenient to refer the supersonic results for a given wing to a transformed wing at a reference Mach number of  $M^2 = 2$ . If this transformation is used a rule resembling the Prandtl-Glauert rule (reference 3) for the subsonic case, where  $M = 0$  is the reference Mach number, may be obtained. This rule may be stated as follows:

The streamline field of the supersonic flow for a given body at a stream Mach number  $M$  may be calculated by multiplying the given  $y$ - and  $z$ -dimensions, including those for the Mach lines, by the factor  $\sqrt{M^2 - 1}$  and then by calculating the flow about the resulting transformed body at the Mach number  $\sqrt{2}$ . The pressure  $p$  and velocity increments  $u$  for the given body at the Mach number  $M$  can then be obtained by multiplying the calculated pressure  $p$  and velocity increments  $u$  at corresponding points of the transformed body by the factor  $\frac{1}{M^2 - 1}$ .

It is interesting to note that the derivation of formulas (13) to (15) as given in this paper corresponds to utilizing the solution for a transformed wing for the whole family of wings related to this transformation and then applying the aforementioned modified Prandtl-Glauert rule.

## RESULTS AND DISCUSSION

Variation of section drag coefficient along span.- Figure 2, which was introduced previously to illustrate the system of Mach lines, also shows the variation of section drag coefficient  $c_d$  along the span. The data are presented for a wing of  $45^\circ$  sweepback and thickness ratio of 0.10. Figure 2(a) gives the results for a wing of infinite aspect ratio and figure 2(b) gives the results for a wing of finite span.

In figure 2(a), the data are shown for Mach numbers of 1.100, 1.343, and 1.414. The lowest Mach number 1.100 represents a case in which the wing leading edge diverges rapidly from the Mach line (upper part of fig. 2(a)). In this case, the section drag coefficient  $c_d$  has a maximum value of 0.0542 at the center section, then drops sharply to zero at a distance of 1.13 chords from the center line. Beyond this point, the wing shows a negative drag, which approaches asymptotically the subsonic value of zero at an infinite distance from the wing center. This type of wave-drag distribution is similar to that indicated in figure 11 of reference 1 for a wing of  $60^\circ$  sweepback at a Mach number of 1.4.

For the higher Mach number 1.343, the spanwise variation of  $c_d$  is markedly flatter. Unlike the preceding case, the drag coefficient does not have its maximum value at the center section but, at first, increases in the outboard direction, then reaches a peak and falls to zero at a distance from the center of 6.6 chords (not shown in fig. 2(a)).

At the highest Mach number 1.414, the Mach line becomes coincident with the wing leading edge. In this case, the wing gives a very high drag and the section drag coefficient increases in the outboard direction, approaching infinity at an infinite distance from the wing center.

Figure 2(b) illustrates the condition at which the aspect ratio is less than  $1/\sqrt{M^2 - 1}$ . The calculated case shown is for an aspect ratio of 1.86 and Mach number of 1.10. In this case, the two wing tips cause increments in section drag coefficient on each half of the wing, namely,  $\Delta c_{dI}$  and  $\Delta c_{dII}$ . The tip effect  $\Delta c_{dI}$  at a given distance from the tip is independent of the aspect ratio. The tip effect  $\Delta c_{dII}$ , however, is a function of the aspect ratio.

Effect of wing tip on wing-drag coefficient.- Figure 3 shows the typical variation with aspect ratio of the increment in  $C_D$  due to the tip  $\Delta C_D$ . The data are shown for a wing of  $45^\circ$  sweep-back and a thickness ratio of 0.10 for Mach numbers of 1.100, 1.343, and 1.414. The present analysis for the untapered wings indicated that if the aspect ratio is equal to or greater than  $2m/(m\beta + 1)$ , the integrated value of  $\Delta c_{dI}$  over the wing is zero. On this basis, if the aspect ratio of the wing is greater than  $1/\sqrt{M^2 - 1}$ , the total increment in drag contributed by tip is zero. As the aspect ratio is reduced, the tip effect  $\Delta C_{DII}$  which occurs when the aspect ratio is smaller than  $1/\sqrt{M^2 - 1}$ , however, leads to an increase in  $C_D$ . The tip effect  $\Delta C_D$  then reaches a peak value at a certain aspect ratio, but as this aspect ratio is further decreased,  $\Delta C_D$  drops sharply. In this case, at aspect ratios of approximately 0.5,  $\Delta C_D$  becomes zero and assumes large negative values with further reductions in aspect ratio. For applications to very small aspect ratios, however, the theory may require modifications. The data in figure 3 show that as the Mach number is increased, the aspect ratio corresponding to zero value of  $\Delta C_D$  becomes smaller.

The tip effects shown in figure 3 for the wing of  $45^\circ$  sweep-back are similar for other wings of different sweepback at appropriate aspect ratios. The conversion formulas indicated in the section entitled "Analysis" indicate that the aspect-ratio effects for wings of different sweepback correspond qualitatively for equal values of the aspect-ratio parameter  $A \tan \Lambda$ . The Mach numbers for each of the wings differ, however. An aspect ratio of 0.8 (fig. 3) for the wing of  $45^\circ$  sweepback at a Mach number of 1.10 for example corresponds to an aspect ratio of  $0.8 \cot \Lambda$  at a Mach number equal to  $\sqrt{1 + [(1.10)^2 - 1] \tan^2 \Lambda}$  for any other wing of sweepback angle  $\Lambda$ .

Variation of wing-drag coefficient with Mach number, sweepback, and slenderness ratio.- Figure 4 shows the variation of  $C_D$  with  $M'$  for different sweepback angles with constant slenderness ratios. The slenderness ratio represents the ratio of the wing semispan measured along the leading edge to the maximum thickness of the center section. The data are presented for sweepback angles of  $30^\circ$ ,  $45^\circ$ ,  $52.5^\circ$ , and  $60^\circ$  with slenderness ratios of 25 and 50. The wings in figure 4 for the different slenderness ratios and sweepback angles are assumed to have the same wing area and the same profile normal to the wing leading edge. The slenderness ratios are based on a thickness ratio of 0.10 measured in a direction

normal to the wing leading edge. The thickness ratio  $t/c$  measured in the flight direction, therefore, varies with sweepback as  $\cos \Lambda$  or is equal to  $0.1 \cos \Lambda$ . The aspect ratio is reduced with sweepback by the factor  $\cos^2 \Lambda$ . The aspect ratio is related to the slenderness ratio by the formula:

$$A = 0.2 \left( \frac{l}{t} \right) \cos^2 \Lambda$$

The plan forms for the different wings are shown in figure 4.

The results in figure 4 show that, in general, the drag coefficient decreases with increasing sweepback. At Mach numbers for which the Mach lines are appreciably ahead of the wing leading edge, increasing the slenderness ratio or aspect ratio gives important reductions in calculated wave-drag coefficient. At Mach numbers for which the Mach lines approach the wing leading edge ( $M \rightarrow \sec \Lambda$ ), however, short wide wings give appreciable reductions in wave-drag coefficient. The figure also indicates that the highest wave-drag coefficients for the normal range of aspect ratio occur at a Mach number equal to  $\sec \Lambda$ .

Effect of aspect ratio on wing-drag coefficient.- Figure 5 indicates the effect of aspect ratio on the wave-drag coefficient for the wing. The data in figure 5 show the wave-drag-coefficient

parameter  $\frac{C_D \tan \Lambda}{100 (t/c)^2}$  plotted against the aspect-ratio parameter

$A \tan \Lambda$ . These results are shown for various values of the Mach number parameter  $\sqrt{M^2 - 1} \cot \Lambda$ , which correspond to a range of Mach number from 1.0 to the secant of the angle of sweepback, or  $1 \leq M \leq \sec \Lambda$ .

Figure 5 shows that for a given value of the Mach number parameter, the maximum wave-drag coefficient occurs at a definite aspect ratio. For example, if  $\Lambda = 45^\circ$  and  $\sqrt{M^2 - 1} \cot \Lambda = 0.310$  (that is,  $M = 1.05$ ) the maximum value of  $C_D$  occurs at an aspect ratio of 0.85. If the aspect ratio is decreased to values smaller than 0.85,  $C_D$  drops very sharply. Similarly, as the aspect ratio is increased from 0.85,  $C_D$  also decreases. Thus, in general for the Mach number parameter corresponding to  $\sqrt{M^2 - 1} \cot \Lambda = 0.310$  the maximum value of  $C_D$  occurs at an aspect ratio equal to  $0.85 \cot \Lambda$ .

Application of curves of figure 5 to wings of arbitrary sweepback and aspect ratio.- The scale labels and curves of figure 5



apply to the series of wings that may be derived from a basic 10-percent-thick,  $45^\circ$  swept-back wing. The labels express the transformation equations (13) to (15). If  $\Lambda$  is set equal to  $45^\circ$  and  $t/c$  is set equal to 0.10 in these labels to correspond to the basic wing, the ordinates become simply  $C_D$ , the abscissa  $A$  (aspect ratio), and the curve parameter  $\sqrt{M^2 - 1}$ . The results in figure 5 may be applied to all swept-back wings covering a range of aspect ratio from 0 to  $10 \cot \Lambda$  corresponding to a range of Mach number from 1.0 to  $\sec \Lambda$ . The data apply specifically to untapered wings with biconvex profiles at zero lift with the wing tips cut off in the direction of flight. The results, however, may be applied to indicate approximate results for profiles similar to the biconvex.

The following example is given in order to illustrate the use of figure 5. For a given wing

$$\Lambda = 70^\circ$$

$$A = 3$$

$$\frac{t}{c} = 0.08$$

$$M = 2.20$$

In order to find  $C_D$ :

$$A \tan \Lambda = 8.24$$

$$\sqrt{M^2 - 1} \cot \Lambda = 0.715$$

From figure 5, for  $A \tan \Lambda = 8.24$  and  $\sqrt{M^2 - 1} \cot \Lambda = 0.715$

$$\frac{C_D \tan \Lambda}{100 (t/c)^2} = 0.0123$$

therefore

$$C_D = 0.00286$$

Comparison of theory with experimental results.- Figure 6 shows a comparison of the theoretical results for wave-drag coefficient with data obtained from unpublished tests made at the Langley Laboratory for swept-back wings attached to a freely falling body. The comparison is shown for a wing of  $45^\circ$  sweepback for two aspect ratios at zero lift. The aspect ratios for the experimental wings based on over-all span were 3.6 and 5.4. Because of the small thickness of the wing section relative to the thickness of the fuselage (0.72 in. to 10.75 in.), the calculations assumed that the fuselage acted as a perfect reflection plane. On this basis, the aspect ratios of 3.6 and 5.4 corresponded to aspect ratios of 2.65 and 4.42. The experimental wing had an NACA 65-009 profile taken in the direction normal to the wing leading edge or a thickness ratio of 0.0636 in the flight direction; whereas, the calculated results are based on a biconvex having the same maximum thickness ratio as the experimental profile. The calculated drag coefficient  $C_D$  was obtained by adding the skin-friction drag coefficient of 0.0027 to the calculated wave-drag coefficient. This value of 0.0027 for the skin-friction drag coefficient was obtained as the minimum drag coefficient from the unpublished experimental results and this value appears somewhat low. The comparison is shown for a range of Mach number from 1.0 to 1.25. The plan form of the wings are shown in figure 6.

The comparison in figure 6 indicates that the calculated values of the wave-drag coefficients are of the order of magnitude of the experimental results. The agreement appears to be closer for the wing of higher aspect ratio than for the wing of smaller aspect ratio. It should be noted that in addition to the approximations inherent in the linearized theory, the calculations do not take account of factors such as fuselage interference, boundary-layer effects, and the exact profile.

#### CONCLUDING REMARKS

A theoretical investigation has been made of the supersonic wave drag of untapered swept-back wings at zero lift. The wing section was biconvex and the wing tip was considered to be cut off

in the direction of flight. The investigation was limited to a range of stream Mach number from 1.0 to a value corresponding to that at which the Mach line coincided with the wing leading edge. For this range of Mach number, the following conclusions have been drawn:

1. In general, the calculated wave-drag coefficient decreased with increasing sweepback.

2. At Mach numbers for which the Mach lines are appreciably ahead of the wing leading edge, increasing the slenderness ratio or aspect ratio gave important reduction in the calculated wave-drag coefficient.

3. At Mach numbers for which the Mach lines approach the wing leading edge (Mach numbers approaching a value equal to the secant of the angle of sweepback), decreasing the slenderness ratio or aspect ratio reduced the calculated wave-drag coefficient.

4. The highest calculated wave-drag coefficients for the normal range of aspect ratio occurred at a Mach number equal to the secant of the angle of sweepback.

5. The maximum wave-drag coefficient occurred at a definite aspect ratio which is determined by the Mach number and angle of sweepback.

6. For aspect ratios greater than  $1/\sqrt{M^2 - 1}$ , where  $M$  is the Mach number, the increment in wave-drag coefficient for the wing contributed by the tip was zero.

7. The variation of the drag with Mach number obtained for one sweepback angle for appropriate aspect ratios may be presented in a unified form so that the drag for the complete range of sweepback angle, aspect ratio, and Mach number may be directly determined from a single chart.

8. A comparison of the theory for a Mach number range from 1.0 to 1.25 with results obtained from tests of swept-back wings attached

to a freely falling body indicated that the calculated values were of the order of magnitude of the experimental results.

Langley Memorial Aeronautical Laboratory  
National Advisory Committee for Aeronautics  
Langley Field, Va.

## APPENDIX A

FORMULAS FOR THE INTEGRAND  $u$  IN EQUATION (3) FOR FINITE  
UNTAPERED SWEEP-BACK WINGS OF BICONVEX PROFILE

$$\text{AT ZERO LIFT} \quad \left[ m = \cot \Lambda \leq \frac{1}{\beta} \right]$$

In order to satisfy the boundary condition for a finite swept-back wing of biconvex profile, the integrand  $u$  in equation (3) may be expressed in terms of components caused by elementary source lines as follows:

$$\begin{aligned}
 u &= u_{0,0} + u_{c,0} + \bar{u}_{0,0} + \bar{u}_{c,0} \\
 &- \left( \frac{1}{D} u_{0,0} - \frac{1}{D} u_{c,0} + \frac{1}{D} \bar{u}_{0,0} - \frac{1}{D} \bar{u}_{c,0} \right) \\
 &- \left[ u_{h/m,h} + \bar{u}_{h/m,-h} - \left( \frac{1}{D} u_{h/m,h} + \frac{1}{D} \bar{u}_{h/m,-h} \right) \right] \quad (A1)
 \end{aligned}$$

where the subscript notation indicates the origin of the source line. The bars over  $u$  refer to the source lines caused by the opposite wing panel; that is,  $\bar{u}$  indicates a source line with a reversal in the sign of  $m$ .

In equation (A1), the  $u$ -functions are given by the real parts of the following expressions:

$$\begin{aligned}
 u_{\xi,\eta}(x,y) &= I \cosh^{-1} \frac{x - \xi - m\beta^2(y - \eta)}{\beta |y - \eta - m(x - \xi)|} \\
 \bar{u}_{\xi,\eta}(x,y) &= I \cosh^{-1} \frac{x - \xi + m\beta^2(y - \eta)}{\beta |y - \eta + m(x - \xi)|}
 \end{aligned}$$

where  $\xi, \eta$  represents the origin of the elementary source lines. For the biconvex profile,

$$\frac{dz}{dx} = \frac{t}{c}$$

and from equation (5), the factor

$$I = \frac{2^t V}{c \pi} \frac{m}{\sqrt{1 - m^2 \beta^2}}$$

The symbol  $\frac{1}{D}$  in equation (A1) refers to an integration operation which represents the influence of the uniform distribution of sink lines along the chord of the biconvex profile. This symbol is defined by the following expressions:

$$\begin{aligned} \frac{1}{D} u_{\xi, \eta}(x, y) &= \int_{x-\beta y}^{+0} \frac{dI}{d\xi} \cosh^{-1} \frac{x - \xi - m\beta^2(y - \eta)}{\beta|y - \eta - m(x - \xi)|} d\xi \\ &= (y - \eta) \frac{dI}{dx} \left\{ \frac{\sqrt{1 - m^2 \beta^2}}{m} \cosh^{-1} \frac{x - \xi}{\beta|y - \eta|} \right. \\ &\quad \left. - \frac{1}{m} \left[ 1 - \frac{m(x - \xi)}{y - \eta} \right] \cosh^{-1} \frac{\frac{x - \xi}{\beta(y - \eta)} - m\beta}{\left| 1 - \frac{m(x - \xi)}{y - \eta} \right|} \right\} \end{aligned} \tag{A2}$$

where, for a biconvex profile

$$\frac{dI}{dx} = -\frac{V}{\pi} \frac{m}{\sqrt{1 - m^2\beta^2}} \frac{d^2z}{dx^2}$$

$$= \frac{4}{c} (t/c) \frac{V}{\pi} \frac{m}{\sqrt{1 - m^2\beta^2}}$$

Equation (A2) may be expressed as a function of  $\frac{x - \xi}{y - \eta}$ , that is

$$\frac{1}{D} u_{\xi, \eta}(x, y) = (y - \eta) f\left(\frac{x - \xi}{y - \eta}\right)$$

Then

$$\frac{1}{D} u_{\xi, \eta}(x, y) = -(y - \eta) f\left[\frac{x - \xi}{-(y - \eta)}\right]$$

The limits of integrations with regard to  $x$  for the section drag coefficients and with regard to  $y$  for the total wing-drag coefficients are discussed. The  $u$ -components caused by each of the elementary source lines are zero at all points outside of the respective Mach cones. The functions for the  $u$ -integrand in equation (3) are therefore evaluated along the section for values of  $x$  beginning at the forward boundary of the Mach cone. This integration gives the section-drag-coefficient components. Similarly, in order to obtain the wing-drag coefficient, the section drag coefficient components obtained from the respective  $u$ -functions are evaluated along the wing span for values of  $y$  contained within the Mach cone. The following table refers to one side of the wing ( $x$  and  $y$  positive) and shows the limits of integration for  $x$  and  $y$  for the required  $u$ -functions:

u-components	Limits of integration			
	x		y	
	Lower limit	Upper limit	Lower limit	Upper limit
$u_{0,0}$ $\bar{u}_{0,0}$ $\frac{1}{D}u_{0,0}$ $\frac{1}{D}\bar{u}_{0,0}$	$y/m$	$\frac{y}{m} + c$	0	h
$u_{c,0}$ $\bar{u}_{c,0}$ $\frac{1}{D}u_{c,0}$ $\frac{1}{D}\bar{u}_{c,0}$	$y\beta + c$	$\frac{y}{m} + c$	0	h
$u_{h/m,h}$ $\frac{1}{D}u_{h/m,h}$	$\frac{h}{m}(m\beta + 1) - y\beta$	$\frac{y}{m} + c$	$h - \frac{mc}{m\beta + 1}$ (if $A > \frac{2m}{m\beta + 1}$ ) 0 (if $A \leq \frac{2m}{m\beta + 1}$ )	h
$\bar{u}_{h/m,-h}$ $\frac{1}{D}\bar{u}_{h/m,-h}$	$y\beta + \frac{h}{m}(m\beta + 1)$	$\frac{y}{m} + c$	$\frac{h(m\beta + 1) - mc}{1 - m\beta}$ (if $A > \frac{2m}{m\beta + 1}$ ) 0 (if $A \leq \frac{2m}{m\beta + 1}$ )	h



## APPENDIX B

FORMULAS FOR WAVE-DRAG COEFFICIENTS FOR FINITE UNTAPERED  
SWEPT-BACK WINGS OF SYMMETRICAL BICONVEX PROFILE

$$\text{AT ZERO LIFT} \quad \left[ m = \cot \Lambda \leq \frac{1}{\beta} \right]$$

## Section Drag Coefficients

In the following analysis the quantities  $y$  and  $K$  are employed nondimensionally in terms of the semichord. The equations for the drag coefficients in all cases refer to the real parts of the indicated expressions.

Section drag coefficients without tip effect.— The section drag coefficient for the given wing at a spanwise position  $y$  and Mach number  $M$  without the tip effect was found to be as follows:

The term  $\frac{2m}{1 - m\beta}$  represents a convenient integration limit which indicates the intersection of the Mach line from the center-section trailing edge with the wing leading edge. For  $y = Km < \frac{2m}{1 - m\beta}$

$$\begin{aligned}
 c_{d_{\infty}}(y) = & \frac{8}{\pi} \left( \frac{t}{c} \right)^2 m \left( K^3 \left( \cosh^{-1} \frac{K+2}{Km'} - 2 \cosh^{-1} \frac{1}{m'} \right) \right. \\
 & + \frac{1}{3\sqrt{1-m'^2}} \left\{ 2 \cosh^{-1} \frac{K(1-m'^2)+2}{2m'} \right. \\
 & - 2(2K^3 - 3K - 1) \cosh^{-1} \frac{K(1+m'^2)+2}{2m'(K+1)} \\
 & + 4K(2K^2 - 3) \cosh^{-1} \frac{1+m'^2}{2m'} + K^2 \left[ 2K(1-m'^2) \right. \\
 & \left. \left. - \sqrt{(1-m'^2) [(K+2)^2 - (Km')^2]} \right] \right\} \left. \right) \quad (B1a)
 \end{aligned}$$

For  $y = Km > \frac{2m}{1 - m\beta}$ , the following expression is added to equation (B1a).

$$\frac{8}{\pi} \left(\frac{t}{c}\right)^2 m \left\{ K^3 \cosh^{-1} \frac{K - 2}{Km'} - \frac{1}{3\sqrt{1 - m'^2}} \left[ 2 \cosh^{-1} \frac{K(1 - m'^2) - 2}{2m'} + 2(2K^3 - 3K + 1) \cosh^{-1} \frac{K(1 + m'^2) - 2}{2m'(K - 1)} + K^2 \sqrt{(1 - m'^2) [(K - 2)^2 - (Km')^2]} \right] \right\} \quad (B1b)$$

where  $m' = m\beta$ .

For the special case  $m = \frac{1}{\sqrt{M^2 - 1}}$ , the Mach line coincides

with the wing leading edge, and the expression for the drag coefficient obtained as a limiting case ( $m' \rightarrow 1$ ) for all values of  $y$  becomes:

$$c_{d_\infty}(y) = \frac{8}{\pi} \left(\frac{t}{c}\right)^2 m \left\{ y'^3 \cosh^{-1} \frac{y' + 2}{y'} - \frac{2}{3} \left[ \frac{y'(3y' + 4)(y' - 1) - 2}{\sqrt{y' + 1}} \right] \right\} \quad (B2)$$

where

$$y' = y\beta$$

At the center section, where  $y$  or  $K = 0$ , equation (B1a) becomes:

$$c_{d_{\infty}} = \frac{32}{3\pi} \left(\frac{t}{c}\right)^2 \frac{m}{\sqrt{1 - m^2 \beta^2}} \cosh^{-1} \frac{1}{m\beta}$$

At the center section, for  $y = 0$  and  $m = \frac{1}{\beta}$ , equation (B2) becomes:

$$c_{d_{\infty}} = \frac{32}{3\pi} \left(\frac{t}{c}\right)^2 m$$

Increment in section drag coefficient caused by wing tips.-

The increment in  $c_d$  caused by the tips depends on various factors, such as the sweep angle, aspect ratio, and Mach number. The following types occur in an untapered wing:

I. If the aspect ratio of the wing is equal to or greater than  $1/\sqrt{M^2 - 1}$  each tip affects solely its own half of the wing. In this case the effect of the tip is limited to the region of the wing outboard and rearward of the front Mach line originating from this tip. (See fig. 2(b).) The region of the wing affected is between values of  $y$  from  $h - \frac{2m}{m\beta + 1}$  to  $h$ .

The increment in section drag coefficient at a Mach number  $M$  and spanwise position  $y$  caused by the tip was found to be as follows:

$$\Delta c_{d_I}(y) = \frac{8}{\pi} \left(\frac{t}{c}\right)^2 m \left\{ \frac{y_a'}{12m'^2} \left[ \left( y_a'^2 \frac{2 + m'^2}{m'} \right. \right. \right. \\ \left. \left. - 12m' \right) \cosh^{-1} \frac{y_a' + 2m'}{|m'y_a'|} + (2m' - 3y_a') \sqrt{\left(\frac{y_a'}{m'} + 2\right)^2 - y_a'^2} \right] \\ \left. - \frac{2}{3\sqrt{1 - m'^2}} \cosh^{-1} \frac{(1 - m'^2)y_a' + 2m'}{2m'^2} \right\} \quad (B3)$$

where the subscript a indicates that the x-axis is shifted to the tip section, and  $y_a' = y_a\beta$  and  $m' = m\beta$ . In the plan form of the wing

$$y = h + y_a$$

In equation (B3) values for  $y_a$  may be taken from  $-\frac{2m}{m\beta + 1}$  to 0. When the Mach line is coincident with the leading edge of the airfoil; that is,  $m = \frac{1}{\sqrt{M^2 - 1}}$ , the expression for  $\Delta c_{dI}$  becomes:

$$\Delta c_{dI}(y) = \frac{4}{\pi} \left(\frac{t}{c}\right)^2 m \left[ \frac{y_a'(y_a'^2 - 4)}{2} \cosh^{-1} \frac{y_a' + 2}{|y_a'|} - \frac{\sqrt{y_a' + 1}}{3} (3y_a'^2 - 2y_a' + 4) \right] \quad (B4)$$

II. If the aspect ratio of the wing is less than  $\frac{1}{\sqrt{M^2 - 1}}$ , the tip on the opposite wing contributes an increment in  $c_d$  in addition to that discussed under type I. The increment in  $c_d$  at a section caused by the opposite tip was obtained in the following form:

$$\begin{aligned} \Delta c_{dII}(y) = & \frac{8}{\pi} \left(\frac{t}{c}\right)^2 m \left( \frac{y_b'}{m^3} \left\{ \frac{1}{12} (7y_b' - 10h' - 2m') \sqrt{[y_b' - 2(h' - m')]^2 - (m'y_b')^2} \right. \right. \\ & - \left. \left[ \frac{y_b'^2}{12} (14 + m'^2) - 3h'y_b' + 2h'^2 - m'^2 \right] \left[ \cosh^{-1} \frac{y_b' - 2(h' - m')}{m'y_b'} \right] \right\} \\ & + \frac{2}{3m^3 \sqrt{1 - m'^2}} \left[ 2y_b'^3 - 6y_b'^2 h' + 3y_b' (2h'^2 - m'^2) - 2h'^3 + 3m'^2 h' - m'^3 \right] \\ & \left. \left[ \cosh^{-1} \frac{y_b' (1 + m'^2) - 2(h' - m')}{2m' (y_b' - h' + m')} \right] \right) \quad (B5) \end{aligned}$$

where the subscript  $b$  indicates that the  $x$ -axis is shifted to the opposite tip section, and where  $y_b' = y_b \beta$ ,  $m' = m \beta$ , and  $h' = h \beta$ . In the plan form of the wing

$$y = y_b - h.$$

The limits for  $y_b$  to be used in equation (B5) depend on the value of aspect ratio  $A$  relative to the parameter  $\frac{2m}{m\beta + 1}$ . Thus

(a) If the aspect ratio of the wing is greater than  $\frac{2m}{m\beta + 1}$ , the front Mach line from the opposite tip intersects the trailing edge at a value of  $y_b = \frac{2(h - m)}{1 - m\beta}$  so that values for  $y_b$  in equation (B5) may be taken from  $\frac{2(h - m)}{1 - m\beta}$  to  $2h$  at the tip. (See fig. 2(b).)

(b) If the aspect ratio  $A$  is equal to or less than  $\frac{2m}{m\beta + 1}$ , the front Mach line from the opposite tip intersects the center section and values for  $y_b$  in equation (B5) may be taken from  $h$  to  $2h$ . In this case, the increment in  $\Delta c_d$  discussed under type I is obtained at spanwise positions of  $y_a$  from  $-h$  to  $0$ .

When  $m = \frac{1}{\sqrt{M^2 - 1}}$ , equation (B5) becomes:

$$\Delta c_{d_{II}} = \frac{8}{\pi} \left(\frac{t}{c}\right)^2 m \left\{ y_b' \left[ \frac{1}{12} (7y_b' - 10h' - 2) \sqrt{y_b' - 2(h' - 1)^2 - y_b'^2} \right. \right. \\ \left. \left. - \left( \frac{5}{4} y_b'^2 - 3h'y_b' + 2h'^2 - 1 \right) \left( \cosh^{-1} \frac{y_b' - 2h' + 2}{y_b'} \right) \right] \right. \\ \left. + \frac{2}{3} \frac{[2y_b'^3 - 6y_b'^2 h' + 3y_b'(2h'^2 - 1) - 2h'^3 + 3h' - 1] \sqrt{1 - h'}}{\sqrt{y_b' + 1 - h'}} \right\}$$

The total increment in drag coefficient at a section caused by the tips is given by

$$\Delta c_d = \Delta c_{d_I} + \Delta c_{d_{II}}$$

and the total drag coefficient at the section is

$$c_d = c_{d_\infty} + \Delta c_d$$

### Wing-Drag Coefficients

Wing-drag coefficient without tip effects.- If the aspect ratio is equal to or less than  $\frac{2m}{1 - m\beta}$ , the wing-drag coefficient without the tip effect is

$$C_{D_\infty} = \frac{8}{\pi} \left(\frac{t}{c}\right)^2 m \left\{ \frac{A'^2}{12m'^3} \left( 3A' \cosh^{-1} \frac{A' + 2m'}{A'm'} \right. \right.$$


---


$$- 6A' \cosh^{-1} \frac{1}{m'} - \sqrt{A'^2(1 - m'^2) + 4m'(A' + m')}$$

$$+ 2A'\sqrt{1 - m'^2} \left. + \frac{1}{3m'^3\sqrt{1 - m'^2}} \left[ 2m'^3 \cosh^{-1} \frac{A'(1 - m'^2) + 2m'}{2m'^2} \right. \right.$$

$$+ (2m'^3 + 3A'm'^2 - A'^3) \cosh^{-1} \frac{A'(1 + m'^2) + 2m'}{2m'(A' + m')} \left. \right.$$

$$\left. + (2A'^3 - 6A'm'^2) \cosh^{-1} \frac{1 + m'^2}{2m'} \right\}$$

where  $A' = A\beta$  and  $m' = m\beta$

If the aspect ratio is greater than  $\frac{2m}{1 - m\beta}$ , the wing-drag coefficient without tip effect is,

$$C_{D\infty} = \frac{8}{\pi} \left(\frac{t}{c}\right)^2 m \left( \frac{A'^2}{12m'^3} \left[ 3A' \left( \cosh^{-1} \frac{A' + 2m'}{A'm'} + \cosh^{-1} \frac{A' - 2m'}{A'm'} \right) \right. \right. \\ - 6A' \cosh^{-1} \frac{1}{m'} - \sqrt{A'^2(1 - m'^2) + 4m'(A' + m')} \\ - \left. \sqrt{A'^2(1 - m'^2) + 4m'(m' - A')} + 2A' \sqrt{1 - m'^2} \right] \\ + \frac{1}{3m'^3 \sqrt{1 - m'^2}} \left\{ 2m'^3 \left[ \cosh^{-1} \frac{A'(1 - m'^2) + 2m'}{2m'^2} \right. \right. \\ - \left. \left. \cosh^{-1} \frac{A'(1 - m'^2) - 2m'}{2m'^2} \right] \right. \\ + (3A'm'^2 - 2m'^3 - A'^3) \cosh^{-1} \frac{A'(1 + m'^2) - 2m'}{2m'(A' - m')} \\ + (3A'm'^2 + 2m'^3 - A'^3) \cosh^{-1} \frac{A'(1 + m'^2) + 2m'}{2m'(A' + m')} \\ \left. \left. + (2A'^3 - 6A'm'^2) \cosh^{-1} \frac{1 + m'^2}{2m'} \right\} \right)$$

Increment in wing-drag coefficient caused by wing tips. - If the aspect ratio of the wing is equal to or greater than  $1/\beta$ , the contribution of the wing tips to the wing-drag coefficient is zero.

If the aspect ratio of the wing is equal to or greater than  $\frac{2m}{m\beta + 1}$ , the total increment in  $C_D$  caused by the local tip, or  $\Delta C_{D_I}$ , is zero; and the increment  $\Delta C_D$  is obtained solely from the effect of the tip located on the opposite half of the wing, or  $\Delta C_{D_{II}}$ . For this case, integration of equation (B5) over the wing yields:

$$\Delta C_D = \frac{8}{\pi} \left(\frac{t}{c}\right)^2 m \left\{ \frac{1}{3m^3 \sqrt{1 - m'^2}} \left[ (A' - 2m')(A' + m')^2 \cosh^{-1} \frac{m'A' + 1}{A' + m'} \right. \right. \\ \left. \left. + (A' + 2m')(A' - m')^2 \cosh^{-1} \frac{1 - m'A'}{|A' - m'|} \right] \right. \\ \left. + \frac{A'}{3m^3} \left[ 6m'^2 - A'^2(2 + m'^2) \right] \cosh^{-1} \frac{1}{A'} - \frac{A'}{3m^3} \sqrt{1 - A'^2} \right\}$$

If the aspect ratio of the wing is less than  $\frac{2m}{m\beta + 1}$ , the increment  $\Delta C_D$  is affected by both wing tips. For this case, integration of equations (B3) and (B5) yields:

$$\Delta C_D = \frac{8}{\pi} \left(\frac{t}{c}\right)^2 m \left( \frac{1}{3m^3 \sqrt{1 - m'^2}} \left[ (A' - 2m')(A' + m')^2 \cosh^{-1} \frac{m'A' + 1}{A' + m'} \right. \right. \\ \left. \left. + (A' + 2m')(A' - m')^2 \cosh^{-1} \frac{1 - m'A'}{|A' - m'|} - 2m'^3 \cosh^{-1} \frac{2m' - A'(1 - m'^2)}{2m'^2} \right. \right. \\ \left. \left. - (2m'^3 - 3m'^2 A' + A'^3) \cosh^{-1} \frac{2m' - A'(1 + m'^2)}{|2m'(m' - A')|} \right] \right. \\ \left. + \frac{A'}{3m^3} \left\{ \left[ 6m'^2 - A'^2(2 + m'^2) \right] \cosh^{-1} \frac{1}{A'} + \frac{A'}{4} \sqrt{4m'(m' - A') + A'^2(1 - m'^2)} \right\} \right. \\ \left. + \frac{A'^3}{4m^3} \cosh^{-1} \frac{2m' - A'}{m'A'} - \frac{A'}{3m^3} \sqrt{1 - A'^2} \right)$$



Total wing-drag coefficient. - The total wing drag is obtained as the sum,

$$C_D = C_{D_\infty} + \Delta C_D$$

where the components  $C_{D_\infty}$  and  $\Delta C_D$  are calculated from the foregoing equations for the wing-drag coefficient appropriate to the aspect ratio of the wing.

Wing-drag coefficient for special case  $m = \frac{1}{\beta}$ . - When the Mach line coincides with the wing leading edge ( $m = \frac{1}{\beta}$ ), the wing-drag coefficient obtained for all aspect ratios as a limiting case ( $m' \rightarrow 1$ ) is equal to the real part of the following expression:

$$C_D = \frac{8}{\pi} \left( \frac{t}{c} \right)^2 m \left( \frac{A'^3}{4} \left( \cosh^{-1} \frac{A'+2}{A'} + \cosh^{-1} \frac{2-A'}{A'} \right) + A'(2-A'^2) \cosh^{-1} \frac{1}{A'} \right. \\ \left. + \frac{1}{6} \left\{ \left[ 3A'^2 + 2A'(1 - 3\sqrt{A'+1}) - 8 \right] \sqrt{1-A'} + (8 + 2A' - 3A'^2) \sqrt{A'+1} \right\} \right)$$

#### Wing-Drag Coefficients at Mach Number of 1.0

The drag coefficient for the wing at  $M = 1.0$  may be expressed in terms of the following formulas which were obtained by integrating over the wing the limiting values for  $c_d$  in equations (B1), (B3),

and (B5) as the factor  $\beta = \sqrt{M^2 - 1}$  approaches zero:

(1) If the aspect ratio of the wing is equal to or greater than  $2m$

$$\begin{aligned}
 C_D = & \frac{8}{3\pi} \left(\frac{t}{c}\right)^2 \frac{m}{h} \left( \int_0^2 m \left[ (-K^3 + 6K + 4) \log_e (K + 2) - 3K^3 \log_e 2K \right. \right. \\
 & + \left. \left. (4K^3 - 6K - 2) \log_e (K + 1) + K^2(K - 2) \right] dK \right. \\
 & + \int_2^{h/m} m \left[ (-K^3 + 6K - 4) \log_e (K - 2) - (K^3 - 6K - 4) \log_e (K + 2) \right. \\
 & + \left. (4K^3 - 6K) \log_e (K^2 - 1) + 2 \log_e \frac{K - 1}{K + 1} - 6K^3 \log_e K \right] dK \\
 & + \int_{h-2m}^h \left\{ \left[ \frac{(y-h)^3}{2m^3} + \frac{3(h-y)}{m} - 2 \right] \left[ \log_e 2(y-h+2m) \right] \right. \\
 & + \left[ \frac{(y+h)^3}{2m^3} + \frac{3y(y^2-h^2)}{m^3} - \frac{3(h+y)}{m} \right] \left[ \log_e m(y+h) \right] \\
 & - \left. \left( \frac{4y^3}{m^3} - \frac{6y}{m} - 2 \right) \left[ \log_e 2m(y+m) \right] \right. \\
 & \left. + \frac{y+h}{4m^3} (7y-3h-2m)(y-h+2m) \right\} dy \tag{B6}
 \end{aligned}$$

where  $K = \frac{y}{m}$

In equation (B6), the first two integrals represent the drag coefficient for the wing without the tip effect; whereas, the last integral represents the effect of the tips  $\Delta C_{D_{II}}$ . For this case, in which the aspect ratio is equal to or greater than  $2m$ , the tip effect  $\Delta C_{D_I}$  is zero; hence the integral for the section increments in  $c_d$  is not given in equation (B6). Equation (B6) has been solved for a sweepback angle of  $45^\circ$  and the results for this sweep angle may be converted to other wings of arbitrary sweepback by the formulas (13) to (15). For the wing of  $45^\circ$  sweepback,  $m = 1$  and  $A \geq 2$ , equation (B6) yields the following result:

$$C_D = \frac{2}{3\pi} \left(\frac{t}{c}\right)^2 \left[ (-A^3 + 12A + 16) \log_e (A + 2) + (-A^3 + 12A - 16) \log_e (A - 2) + 2A(A^2 - 12) \log_e A - 4A \right] \quad (B7)$$

(2) If the aspect ratio of the wing is smaller than  $2m$ , the upper limit of the first integral in equation (B6) is reduced from 2 to  $h/m$ , the second integral vanishes, and the lower limit for the third integral is reduced from  $h - 2m$  to zero. For this case, however, in which the aspect ratio is less than  $2m$ ,  $\Delta C_{D_I}$  is not zero, and the following integral must be added to those in equation (B6) to obtain  $C_D$ :

$$\Delta C_{D_I} = \frac{8}{3\pi} \left(\frac{t}{c}\right)^2 \frac{m}{h} \int_{-h}^{h/m} \left[ \left( \frac{y_a^3}{2m^3} - \frac{3y_a}{m} \right) \log_e \frac{2(y_a + 2m)}{my_a} + 2 \log_e \frac{m^2}{y_a + 2m} + \frac{y_a(2m - 3y_a)(y_a + 2m)}{4m^3} \right] dy_a \quad (B8)$$

where

$$y_a = y - h$$

For the wing of  $45^\circ$  sweepback,  $m = 1$ , and  $A < 2$ , equations (B6) and (B8) yield the same result for  $C_D$  as that obtained for values of  $A$  greater than 2, as expressed by equation (B7). In this case, the real part of  $\log_e(A - 2)$  is used.

## REFERENCES

1. Jones, Robert T.: Thin Oblique Airfoils at Supersonic Speed. NACA TN No. 1107, 1946.
2. Puckett, Allen E.: Supersonic Wave Drag of Thin Airfoils. Jour. Aero. Sci., vol. 13, no. 9, Sept. 1946, pp. 475-484.
3. Göthert, B.: Ebene und räumliche Strömung bei hohen Unterschallgeschwindigkeiten (Erweiterung der Prandtl'schen Regel). Bericht 127 der Lilienthal-Gesellschaft für Luftfahrtforschung, 1940, pp. 97-101.

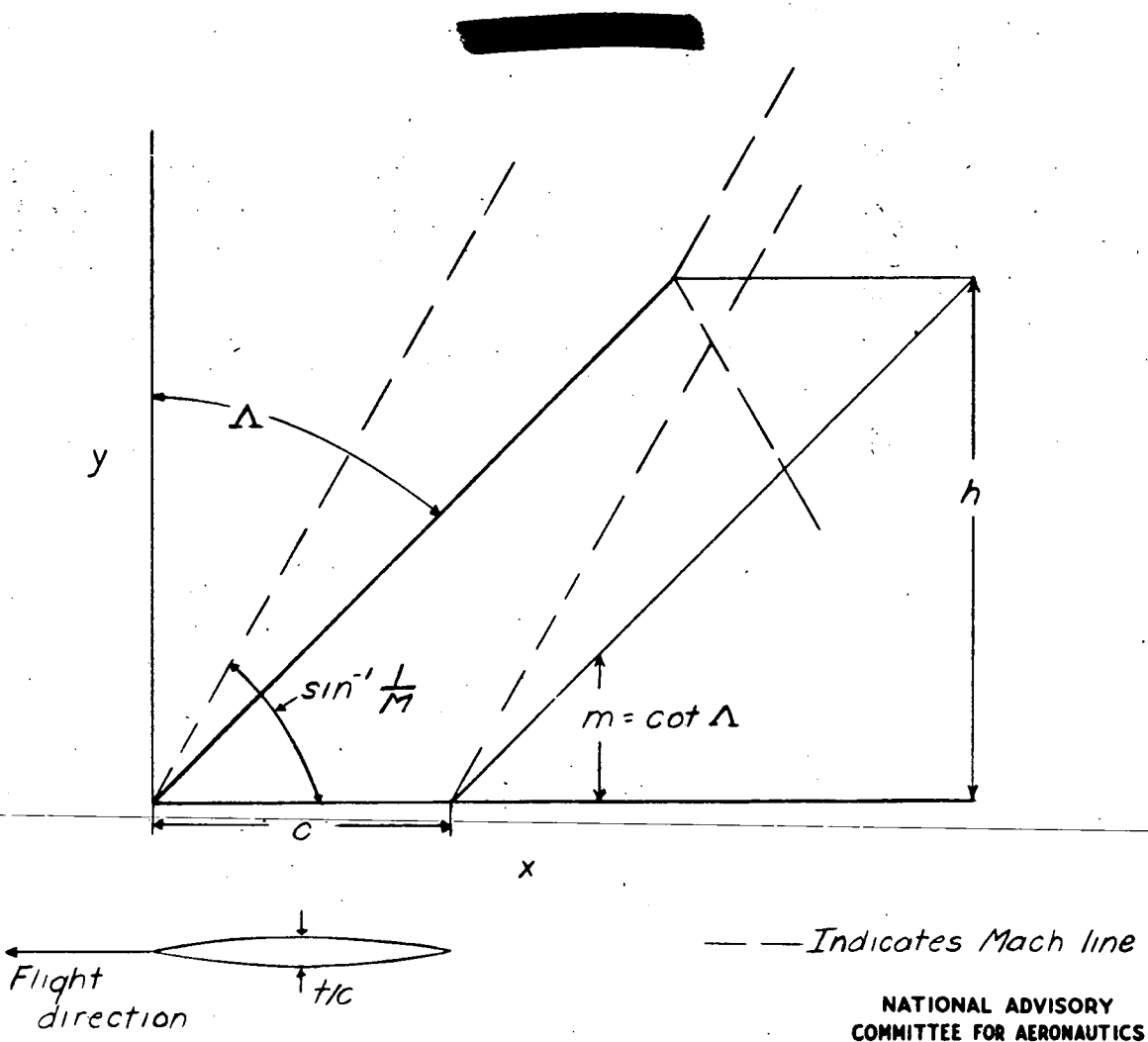
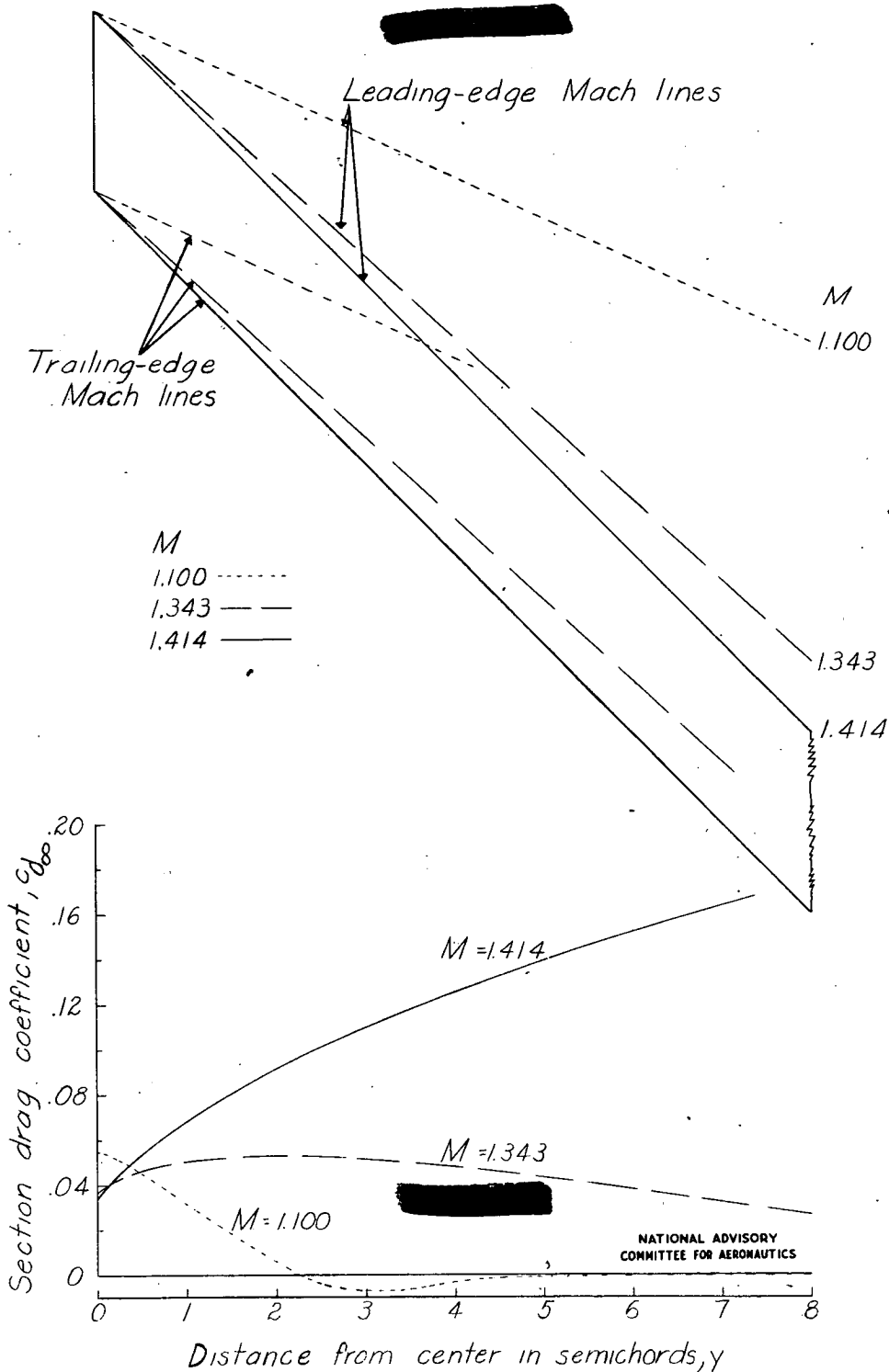


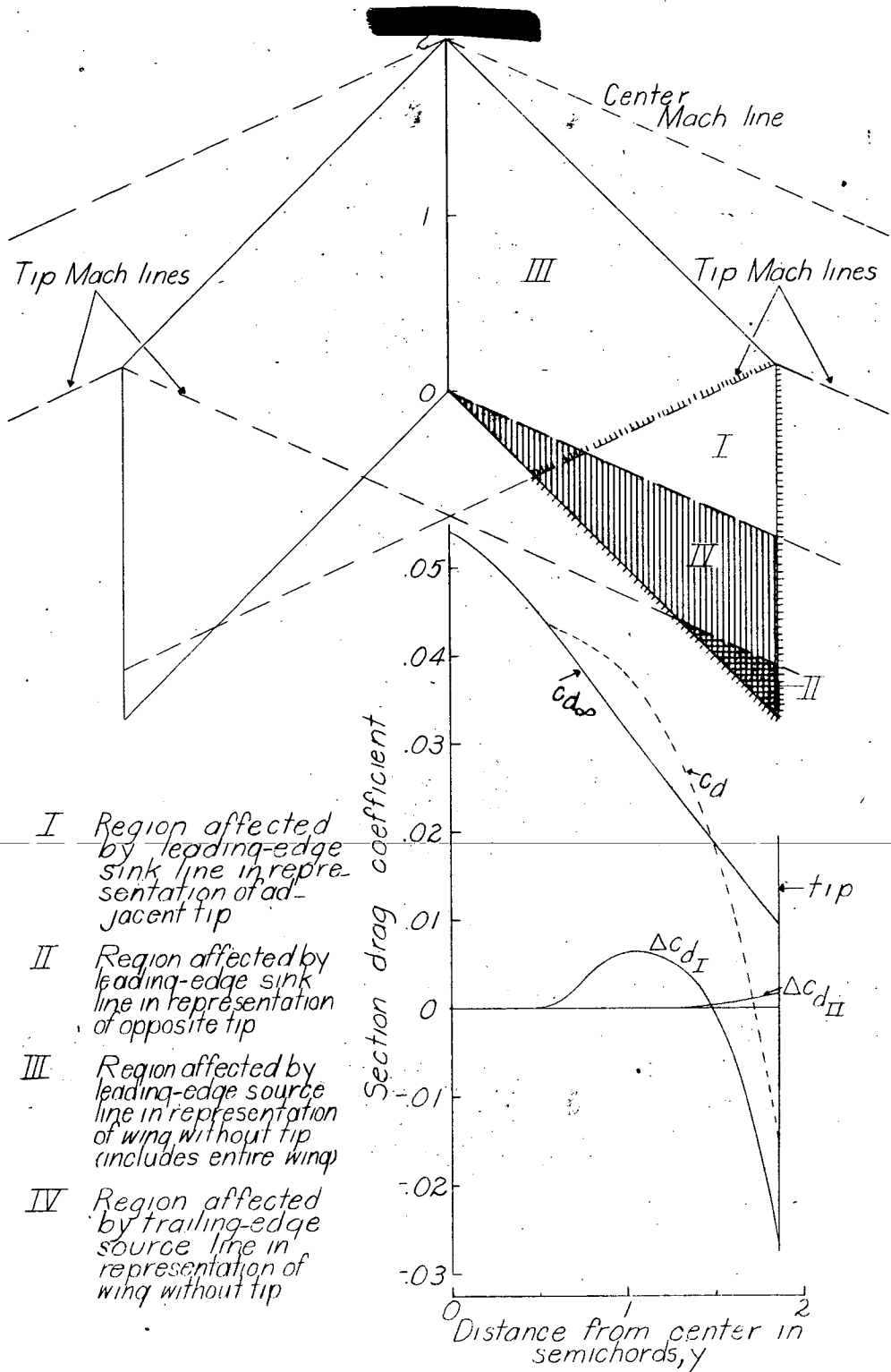
Figure 1. - Symbols for wing plan form.

~~CONFIDENTIAL~~



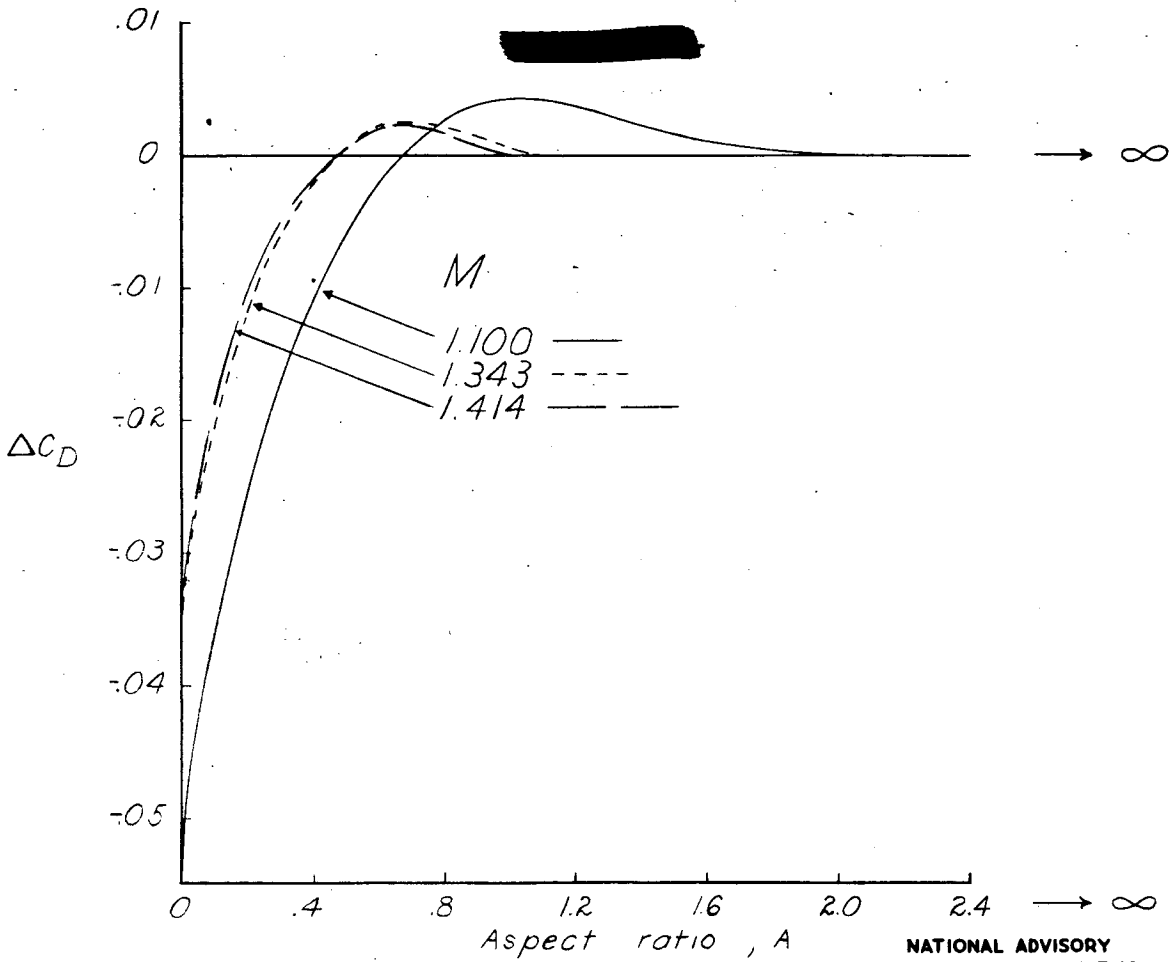
(a) Without tip effect at several Mach numbers.

Figure 2.—Typical distributions of section wave-drag coefficients along wing span. Biconvex profile of zero lift; sweepback angle, 4.5°; thickness ratio in flight direction, 0.10.



(b) With tip effect. Aspect ratio, 1.86; Mach number, 1.10.

Figure 2. —Concluded.



NATIONAL ADVISORY  
COMMITTEE FOR AERONAUTICS

Figure 3.— Typical variations with aspect ratio of the increments in wing wave-drag coefficient caused by wing tips at different Mach numbers. Biconvex profile at zero lift; sweepback angle,  $45^\circ$ ; thickness ratio in flight direction, 0.10.



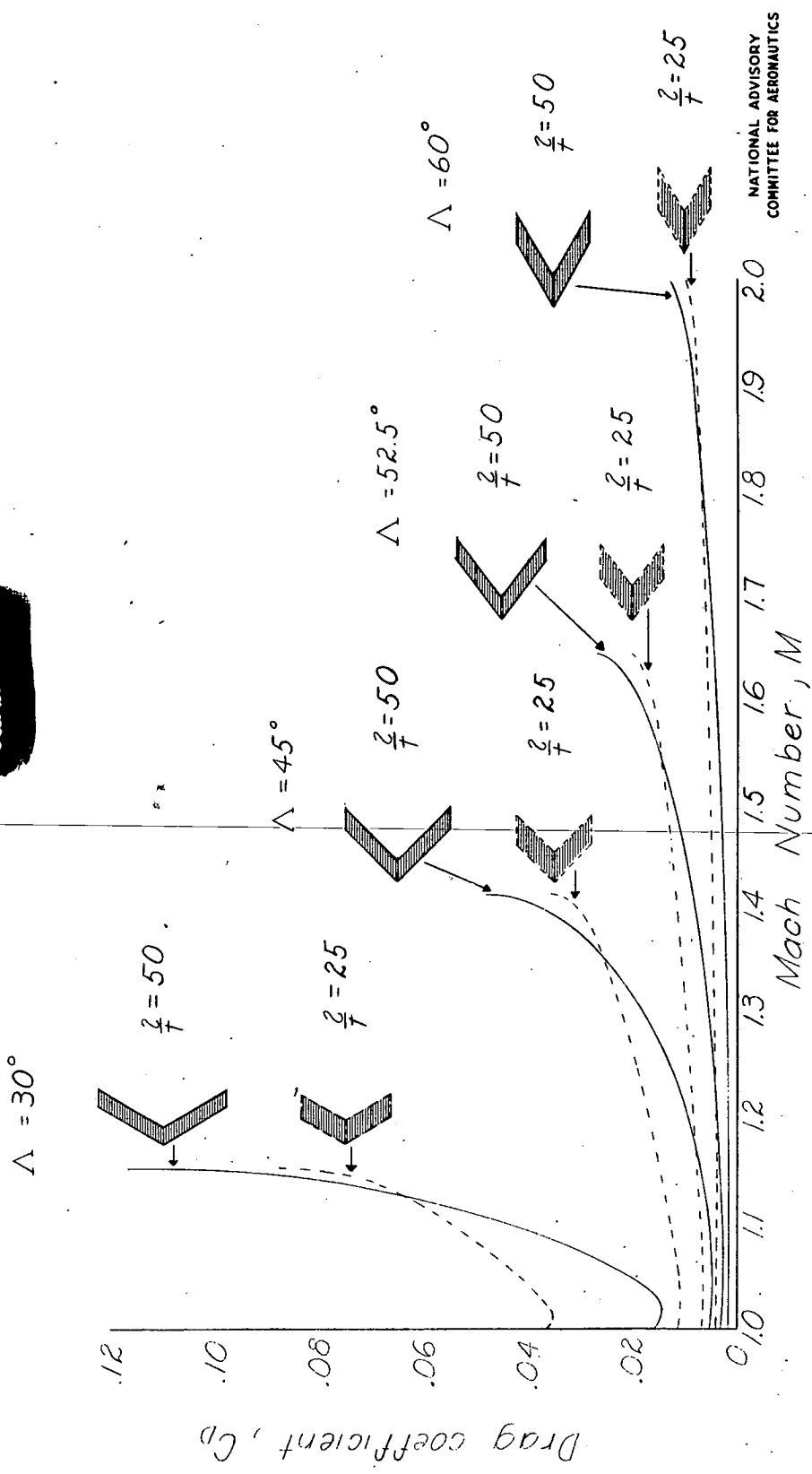
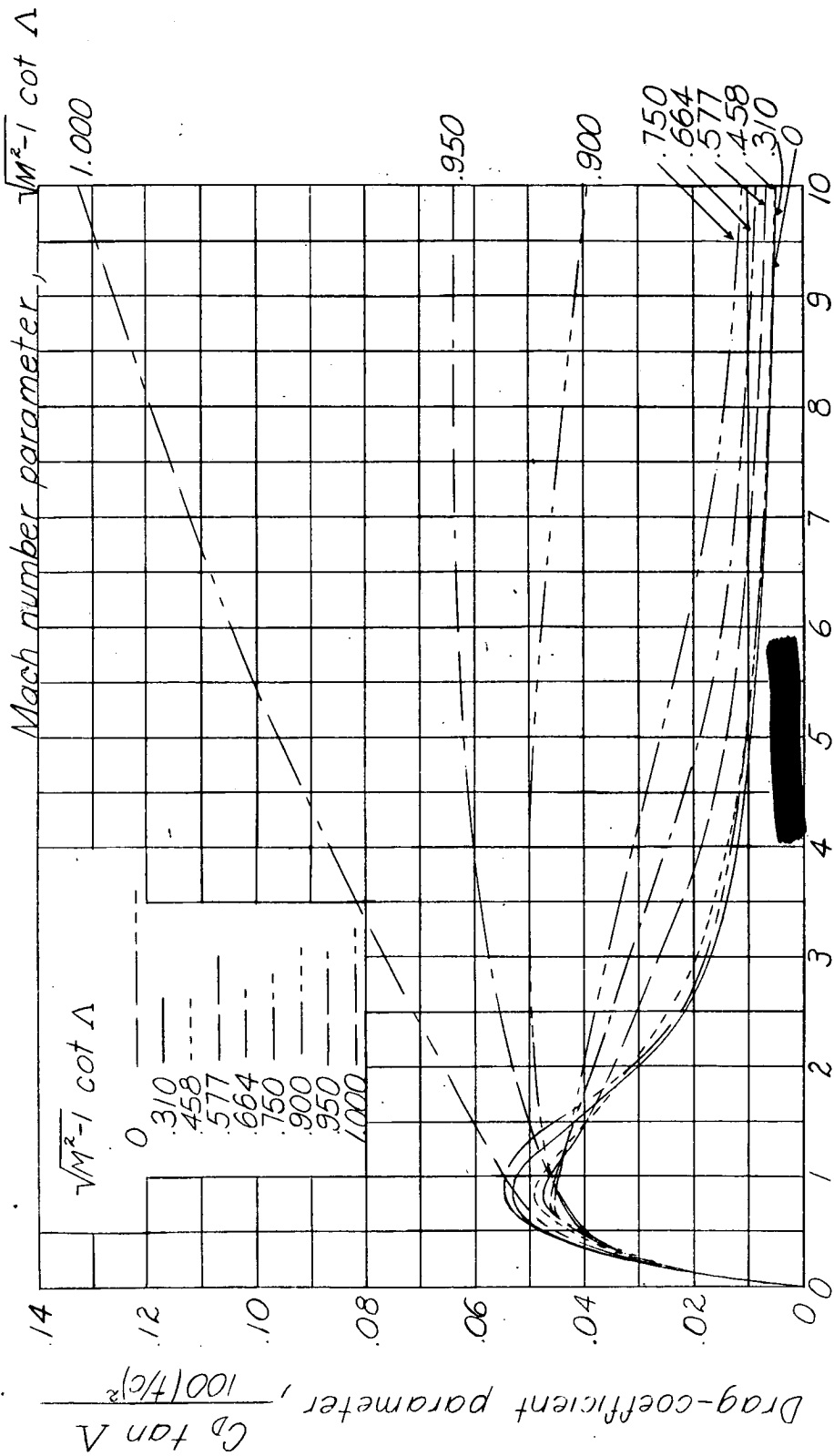


Figure 4. Variation with Mach number of wing wave-drag coefficient for different sweepback angles with constant slenderness ratios. Biconvex profile at zero lift;  $\Lambda = 0.20 \frac{z}{t} \cos^2 \Lambda$ ;  $\frac{z}{t} = 0.10 \cos \Lambda$ ; constant wing area.



NATIONAL ADVISORY  
COMMITTEE FOR AERONAUTICS

Aspect-ratio parameter,  $A \tan \Delta$

Figure 5. — Generalized curves for variation of wing wave-drag coefficient with aspect ratio for constant sweepback angles, Mach numbers, and thickness ratios. Biconvex profile at zero lift.

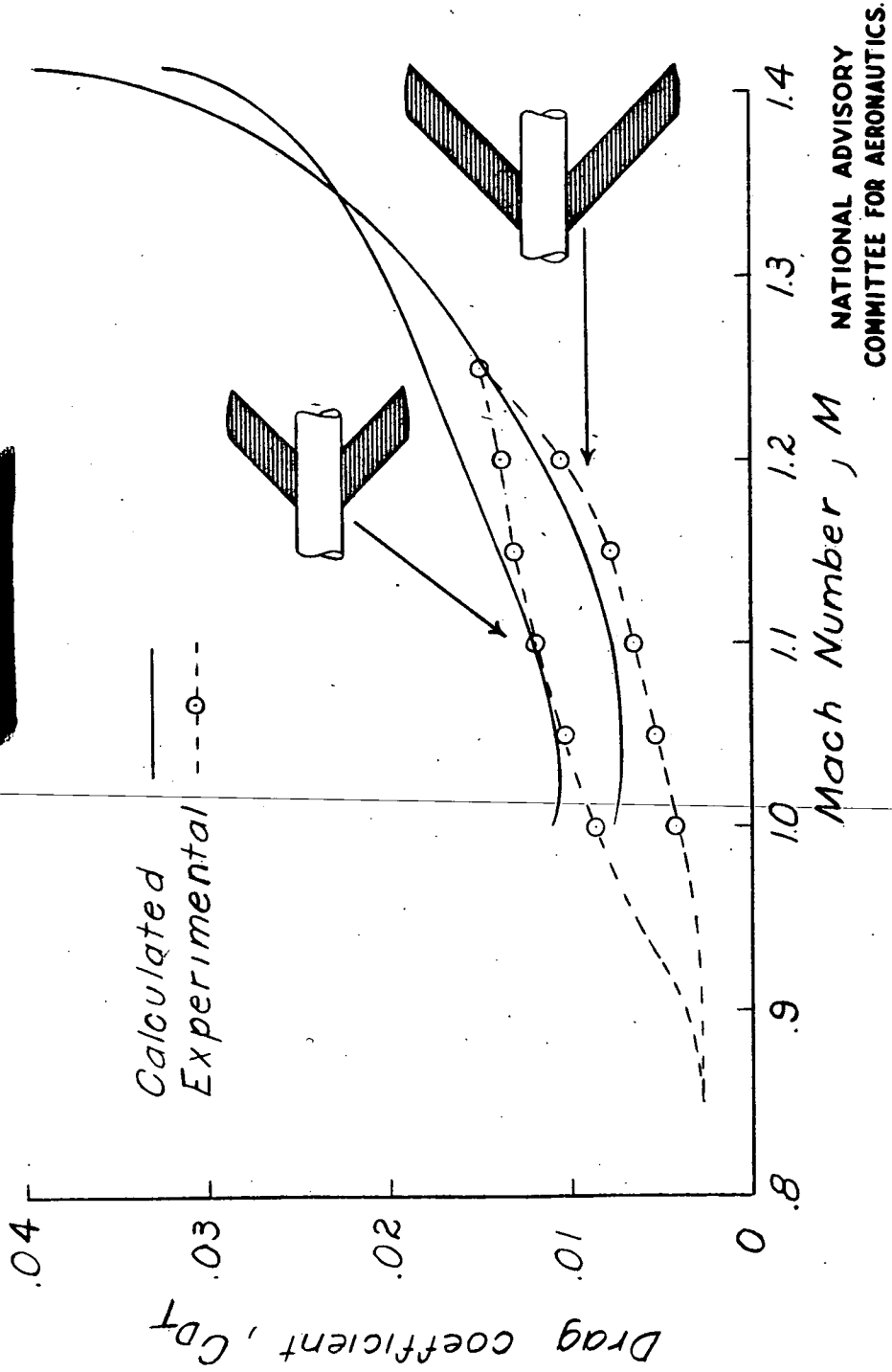


Figure 6.— Comparison of calculated wing wave-drag coefficient with experimental results. Sweepback angle, 45°; thickness ratio in flight direction, 0.0636.

NATIONAL ADVISORY COMMITTEE FOR AERONAUTICS